Energy exchange between a nonlinear absorber and a pendulum under parametric excitation

Gabriel HUREL[1], Alireza TURE SAVADKOOHI[1], Claude-Henri LAMARQUE[1]

[1]Univ. Lyon, ENTPE, LTDS UMR CNRS 5513, F-69518 Vaulx-en-Velin, France
gabriel.hurel@entpe.fr

Abstract

The studied system is a planar pendulum coupled with a nonlinear absorber and parametrically excited at its basis. The dynamical equations are treated with a multiple scale method. At fast time scale, a slow invariant manifold represents the asymptotic behavior. At slow time scale, the equilibrium points and their stability are investigated. Several phase portraits complete the analysis of the dynamical behavior of the system. Finally, numerical examples are given to confirm analytic predictions.

1 Introduction

Vibrations may be problematic in mechanical systems. They can provoke abnormal wear, noise or discomfort especially in case of transportation. Some devices have been designed in order to control these vibrations. Frahm [1] proposed a tuned mass damper i.e. a spring mass device coupled with the main system and able to reduce the energy of one mode. Later on, Roberson [2] showed that a nonlinear behavior of the control device can be more efficient. Since then, several nonlinear absorbers have been designed such as nonlinear tuned vibration absorber (NTVA) [3] or the nonlinear energy sink (NES) [4, 5]. The latter is purely nonlinear i.e. there is no linear term in the restoring force function. Whereas the tuned mass damper is efficient only for one mode, the NES can be used on a wider range of frequency.
Here, the system is a pendulum subject to a parametric excitation corresponding to the vertical displacement of its rotation axis. It corresponds to many industrial systems, in particular to a rope-way vehicle excited by the movement of the cable. Matsuhisa et al. [6] designed several linear and nonlinear tuned mass damper in order to control the oscillations of a pendulum. Song [7] analyzed a parametrically excited pendulum used as a nonlinear absorber with an harmonic balance method. Hurel et al. [8, 9] studied a NES coupled to a two-dof pendulum excited by a generalized force with a multiple scale method. Here, the dynamical behavior of the system is also analysed with a multiple scale method.
In the section 2, the system is presented and dynamic equations are written. These equations are analyzed at two different scales of time in section 3. Then, in section 4, two numerical examples are given to illustrate analytic developments. Finally, the paper is concluded in section 5.

2 Description of the studied system

2.1 Main system

The main system is a pendulum in the plan $(\vec{e}_x, \vec{e}_y)$ attached at the point P by a hinge joint characterized by a viscous damping coefficient C_φ as seen on Fig. 1. Its mass, moment of inertia and center of mass are noted respectively M, J and G. The length L is the distance between the points P and G. The pendulum rotates around the point P with an angle φ. A gravitational field of magnitude g and direction $-\vec{e}_y$ exists.

2.2 Nonlinear absorber

In order to control the oscillations of the pendulum, a nonlinear absorber is coupled to the main system at a distance a from the point P. The mass m of the absorber is very small compared to the mass of the main system.

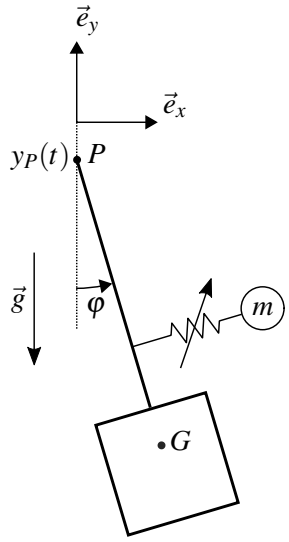

Figure 1 – Parametrically excited pendulum coupled with a nonlinear energy sink.

The ratio of mass is called ε:

$$\varepsilon = \frac{m}{M} \ll 1 \tag{1}$$

The nonlinear force function of the absorber reads:

$$s(u) = Ku^3 + C_u\dot{u} \tag{2}$$

where u is the relative displacement between m and the attached point with the main system and C_u is a viscous damping coefficient.

2.3 Parametric excitation

The main system is subject to a parametric excitation: an imposed vertical displacement of the point P called $y_P(t)$. We assume the displacement small (order of ε) and periodic with a frequency Ω. It can be written as Fourier series:

$$y_P(t) = \varepsilon \sum_{n\in\mathbb{Z}} y_n e^{in\Omega t} \tag{3}$$

where i is the complex number such as $i^2 = -1$.

2.4 Dynamical equations

The coordinates of the center of mass G and the mass of the absorber m read:

$$\begin{cases} x_G = L\sin(\varphi) \\ y_G = y_P - L\cos(\varphi) \end{cases}, \qquad \begin{cases} x_m = a\sin(\varphi) + u\cos(\varphi) \\ y_m = y_P - a\cos(\varphi) + u\sin(\varphi) \end{cases} \tag{4}$$

The kinetic $\mathscr{K}$ and potential $\mathscr{U}$ energies of the system became:

$$\mathscr{K} = \frac{1}{2}J\dot{\varphi}^2 + \frac{1}{2}M\left(\dot{x}_G^2 + \dot{y}_G^2\right) + \frac{1}{2}m\left(\dot{x}_m^2 + \dot{y}_m^2\right) \tag{5}$$

$$\mathscr{U} = Mgy_G + mgy_m + \frac{1}{4}Ku^4 \tag{6}$$

The non-conservative internal forces of the system are:

$$F_\varphi = C_\varphi\dot{\varphi} \tag{7}$$

$$F_u = C_u\dot{u} \tag{8}$$

We deduct from Eqs. 4, 5, 6, 7 and 8 with the Lagrange equations, the dynamic equations of the system:

$$\begin{cases} \left[L+j+\varepsilon(a^2+u^2)\right]\ddot{\varphi}+\varepsilon a\ddot{u}+\varepsilon c_\varphi\dot{\varphi}+2\varepsilon\dot{\varphi}\dot{u}u+\left[L\sin(\varphi)+\varepsilon(a\sin(\varphi)+u\cos(\varphi))\right](g+\ddot{y}_P)=0 \\ \varepsilon\left[a\ddot{\varphi}+\ddot{u}-\dot{\varphi}^2u+c_u\dot{u}+(g+\ddot{y}_P)\sin(\varphi)\right]+ku^3=0 \end{cases} \tag{9}$$

where $j=\dfrac{J}{M}$, $c_\varphi=\dfrac{C_\varphi}{M}$, $c_u=\dfrac{C_u}{m}$ and $k=\dfrac{K}{M}$. The natural frequency ω_0 of the main system alone at small angle reads:

$$\omega_0=\sqrt{\frac{Lg}{j+L^2}} \tag{10}$$

3 Asymptotic behavior

We use a multiple scale method to understand the behavior of the system at several scales of time. To this end, the time t is broken down in several scales τ_n, thanks to the small parameter ε:

$$\tau_n=\varepsilon^n t,\ n\in\mathbb{Z} \tag{11}$$

The derivative operator can be redefined:

$$\frac{\mathrm{d}}{\mathrm{d}t}=\sum_{n\in\mathbb{Z}}\varepsilon^n\frac{\partial}{\partial\tau_n} \tag{12}$$

We assume the angle φ and the displacement u are small. A change of scale can be performed:

$$\varphi=\sqrt{\varepsilon}\overline{\varphi} \tag{13}$$

$$u=\sqrt{\varepsilon}\overline{u} \tag{14}$$

Then the complex variables of Manevitch [10] are introduced:

$$\Phi\mathrm{e}^{i\Omega t}=\dot{\overline{\varphi}}+i\Omega\overline{\varphi} \tag{15}$$

$$U\mathrm{e}^{i\Omega t}=\dot{\overline{u}}+i\Omega\overline{u} \tag{16}$$

In the following development, we keep only the first harmonics thanks to a Galerkin method. This is carried out for an arbitrary function of the system $h(\tau_0,\tau_1,\tau_2,...)$ via:

$$H=\frac{\Omega}{2\pi}\int_0^{\frac{2\pi}{\Omega}}h(\tau_0,\tau_1,\tau_2,...)\mathrm{e}^{-i\Omega\tau_0}\mathrm{d}\tau_0 \tag{17}$$

We assume the frequency of the first harmonic of the excitation Ω is closed to ω_0:

$$\Omega-\omega_0=\sigma\varepsilon \tag{18}$$

3.1 Slow time scale τ_0

At fast time scale τ_0, the Eqs. 9 of the system yield to:

$$\frac{\partial\Phi}{\partial\tau_0}=0 \tag{19}$$

$$\frac{\partial U}{\partial\tau_0}+i\frac{a\omega_0^2-g}{2\omega_0}\Phi+\frac{i\omega_0+c_u}{2}U-i\frac{3k}{8\omega_0^3}|U|U^2=0 \tag{20}$$

We conclude from the Eq. 19 that the amplitude Φ is independent of fast time τ_0. We are looking for the asymptotic state of the system at fast time: $\tau_0\longrightarrow\infty$ and $\frac{\partial U}{\partial\tau_0}=0$. By writing the complex variables in the polar form $\Phi=N_\varphi\mathrm{e}^{i\delta_\varphi}$ and $U=N_u\mathrm{e}^{i\delta_u}$, the Eq. 20 gives:

$$(a\omega_0^2-g)^2N_\varphi^2=\left(\frac{3k}{4\omega_0^2}N_u^3-\omega_0^2N_u\right)^2+c_u^2\omega_0^2N_u^2 \tag{21}$$

The Eq. 21 describes the slow invariant manifold of the system (SIM). It is showed on Fig. 2 with the following parameters: $k = 0.15\,\mathrm{m^{-2}\,s^{-2}}$, $j = 10\,\mathrm{m}$, $L = 1\,\mathrm{m}$, $a = 1\,\mathrm{m}$, $c_u = 0.1\,\mathrm{s^{-1}}$ and $g = 9.81\,\mathrm{m\,s^{-2}}$. By following the method described by Ture Savadkoohi et al. [11] we find two singular points:

$$N_{u1,2} = \frac{2\omega_0^{3/2}\sqrt{2\omega_0 \pm \sqrt{\omega_0^2 - 3c_u^2}}}{3\sqrt{k}} \tag{22}$$

The zone of the SIM between these singular points is unstable.

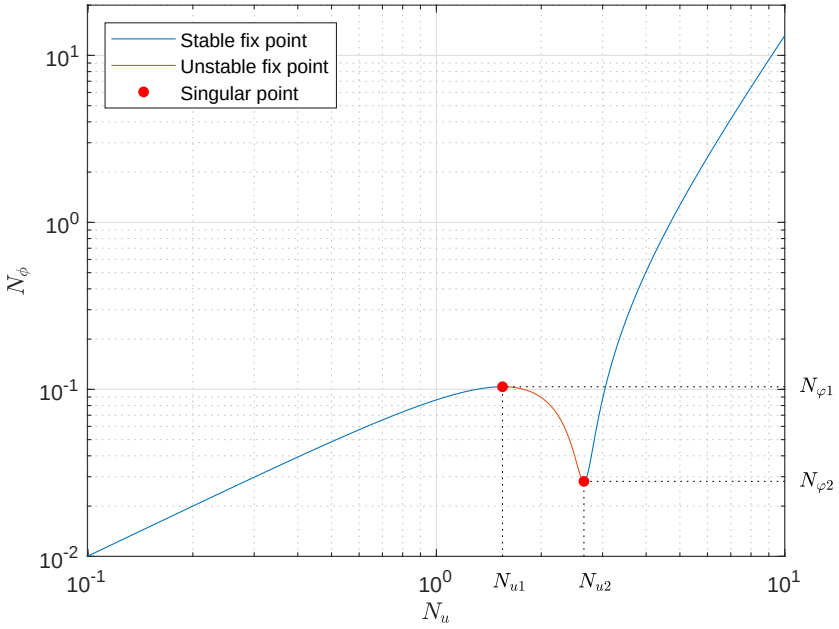

Figure 2 – Slow Invariant Manifold of the system with stable and unstable zones and singular points.

3.2 Fast time scale τ_1

We study now the system at fast time scale around the SIM. The analysis of Eqs. 9 gives:

$$Lg\frac{\partial \Phi}{\partial \tau_1} + \left(i\frac{2\sigma Lg + a\omega_0(a\omega_0^2 - g)}{2} + \frac{c_\varphi \omega_0^2}{2}\right)\Phi + i\frac{\omega_0(a\omega_0^2 - g)}{2}U - 2iy_2 L\omega_0^3\Phi^\star + i\frac{Lg\,|\Phi|^2\,\Phi}{16\omega_0} = 0 \tag{23}$$

The complex variable Φ can be expressed as a function of U thanks to the Eq. 20 of the SIM:

$$\Phi = \frac{U}{a\omega_0^2 - g}\left(\frac{3k\,|U|^2}{4\omega_0^2} - \omega_0^2 + 4ic_u\omega_0\right) \tag{24}$$

To find he equilibrium points, we consider no variation of Φ at fast time i.e. $\frac{\partial \Phi}{\partial \tau_1} = 0$. By replacing Eq. 24 in Eq. 23 and by taking the norm, we obtain a polynomial of degree 9 in N_u^2. The solutions are obtained numerically and represented on Fig. 3 as a function of σ with $c_\varphi = 50\,\mathrm{m\,s^{-1}}$ and $y_2 = 20\,\mathrm{m}$.

The stability of the equilibrium points is determined by a perturbation method with Eqs. 23 and 24:

$$\delta_u \to \delta_u + \Delta\delta_u, \qquad N_u \to N_u + \Delta N_u \tag{25}$$

After linearisation, we can write:

$$\mathbf{A}\begin{bmatrix} \frac{\partial \Delta\delta_u}{\partial \tau_1} \\ \frac{\partial \Delta N_u}{\partial \tau_1} \end{bmatrix} = \mathbf{B}\begin{bmatrix} \Delta\delta_u \\ \Delta N_u \end{bmatrix} \tag{26}$$

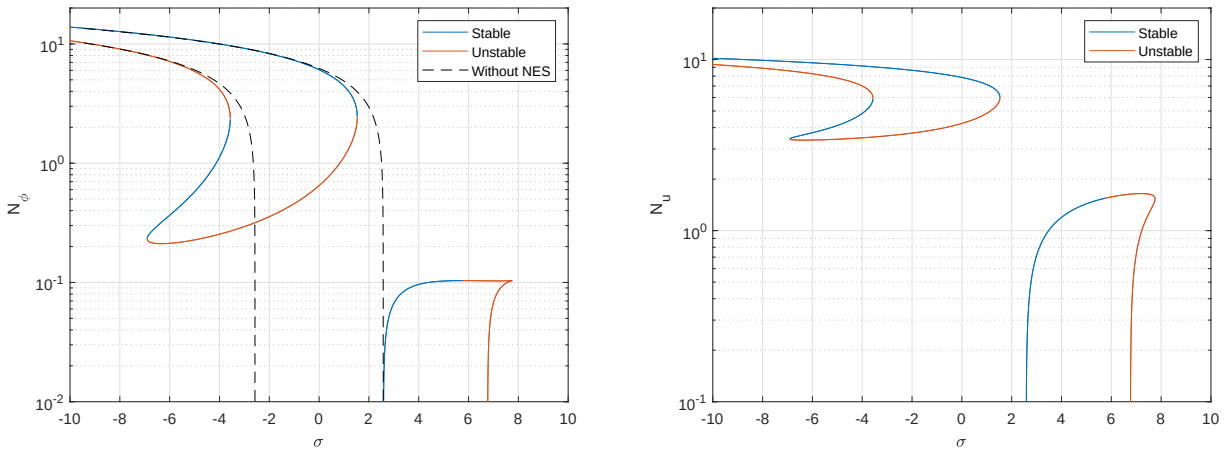

(a) N_φ (b) N_u

Figure 3 – Equilibrium point of the system with NES compared to the equilibrium points of the system without NES (dashed line) as a function of σ.

where $\mathbf{A}$ and $\mathbf{B}$ are matrices. The stability depends on the signs of the eigenvalues of $\mathbf{A}^{-1}\mathbf{B}$. On the Fig. 3, the stability of the equilibrium points is represented with blue (stable) and red (unstable) colors. Note that $N_u = N_\varphi = 0$ is also an equilibrium point for every σ but is not represented because of the logarithmic scale of the graph. Its stability depends on δ_u.

3.3 Phase portrait

The knowledge of the equilibrium points and their stability is not enough to predict the behavior of the system. To complete the analysis, phase portraits are computed and plotted on Fig. 4 for two values of σ. In each case, for a starting point of the system with $N_\varphi(0) < 0.2\,\mathrm{s}^{-1}$, the system will evolute to stay below the second singular point i.e. $\exists t_1, \forall t > t_1\ N_\varphi(t) \leq N_{\varphi 1}$. This fact is illustrated with numerical examples in the next section.

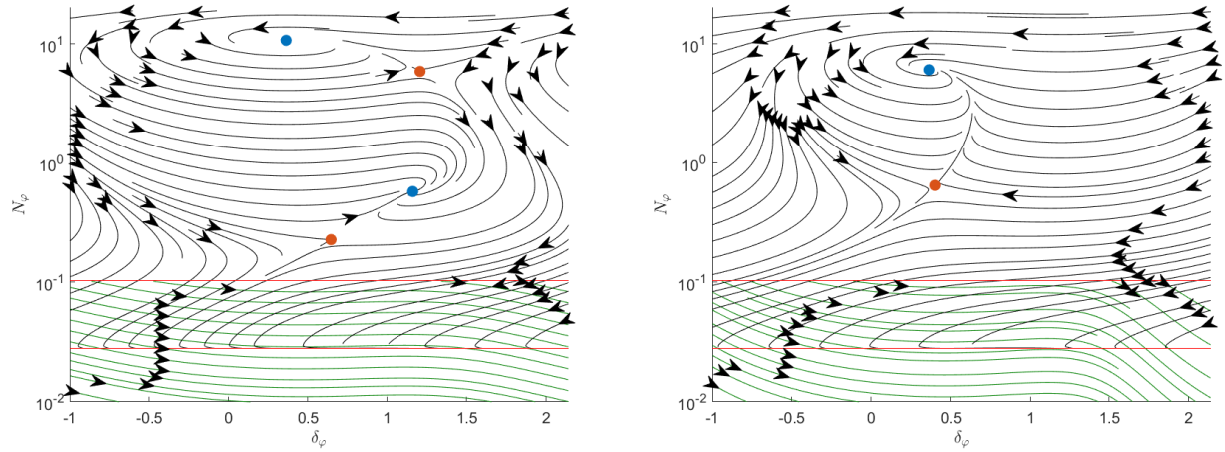

(a) $\sigma = -5\,\mathrm{Hz}$ (b) $\sigma = 0\,\mathrm{Hz}$

Figure 4 – Phase portrait of the system for two values of σ. A blue point is a stable equilibrium point whereas a red point is an unstable equilibrium point. Red lines correspond to singular points $N_{\varphi 1}$ and $N_{\varphi 2}$. The first stable zone of the SIM ($N_u < N_{u1}$) is represented by green curves and the second stable zone ($N_u > N_{u2}$) by black curves. The equilibrium point $N_\varphi = 0$ is not visible because of the logarithmic scale.

4 Numerical simulations

In order to illustrate the efficiency of the NES, two cases are shown with $\sigma = 0\,\mathrm{Hz}$:

- case 1: the pendulum without NES with a very low initial amplitude $N_\varphi(0) = 0.1\,\mathrm{s}^{-1}$ but with a particular phase $\delta_\varphi(0) = 1\,\mathrm{rad}$.
- case 2: the pendulum with NES with a relatively high initial amplitude $N_\varphi(0) = 0.4\,\mathrm{s}^{-1}$ and an arbitrary phase $\delta_\varphi(0) = 1\,\mathrm{rad}$.

The results are shown on figure 5 and 6 with $\varepsilon = 10^{-2}$. First, we note a good agreement between numerical calculations and analytic phase portraits. In the first case, despite the initial amplitude is low, the system moves toward an equilibrium point with high amplitude ($N_\varphi = 0.8$). In the second case, the system goes to the equilibrium point with zero amplitude while the initial condition was higher than in the previous case. This is true for any initial phase angle $\delta_\varphi(0)$.

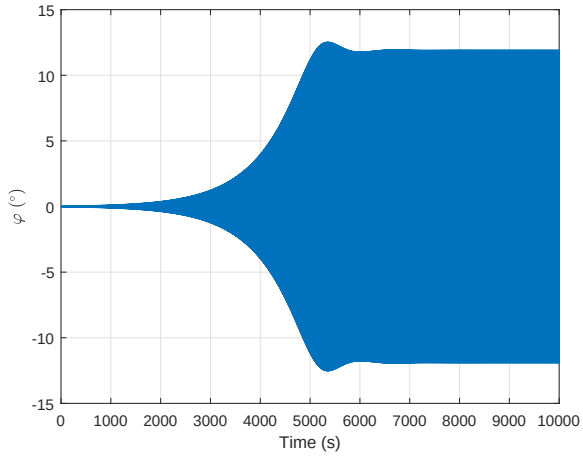

(a) φ as a function of time.

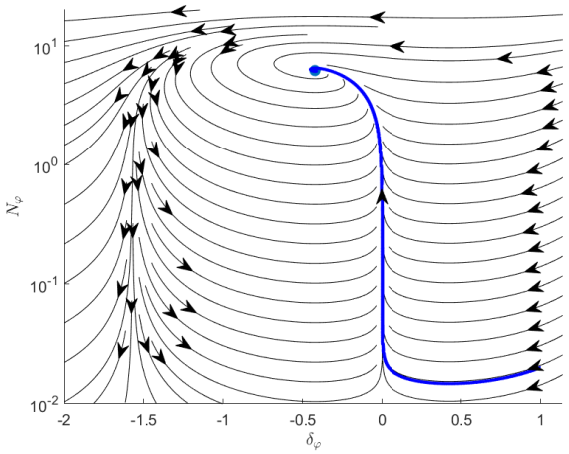

(b) Phase portrait and numerical result.

Figure 5 – Case 1: numerical result without NES, $N_\varphi(0) = 0.1\,\mathrm{s}^{-1}$, $\delta_\varphi(0) = 1\,\mathrm{rad}$

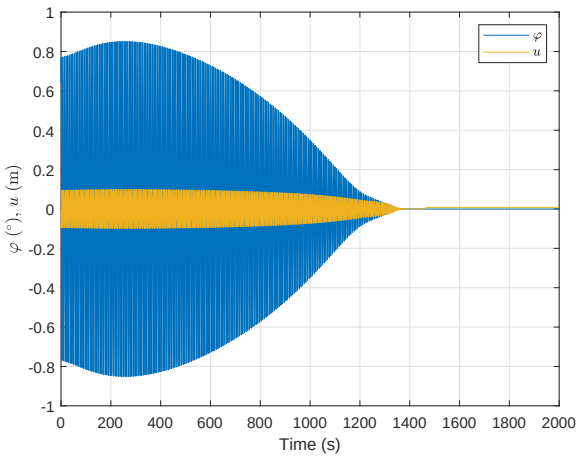

(a) φ and u as functions of time.

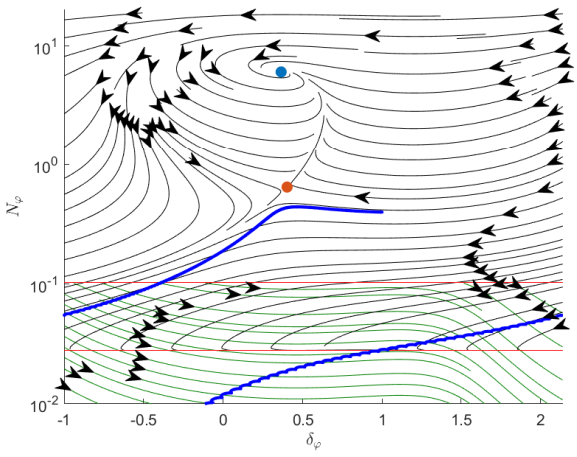

(b) Phase portrait and numerical result.

Figure 6 – Case 2: numerical result with NES, $N_\varphi(0) = 0.4\,\mathrm{s}^{-1}$, $\delta_\varphi(0) = 1\,\mathrm{rad}$

5 Conclusion

After a presentation of a system of a pendulum coupled with a nonlinear energy sink under parametric excitation, the dynamic equations are written thanks to the Lagrange equations. The analysis with a multiple scale method at fast time shows a slow invariant manifold of the system. At the next order, the equations give the equilibrium points and their stability. They are traced as a function of the frequency of excitation. To better predict the behavior of the system, phase portraits are drawn at different values of frequency. They show that the nonlinear energy sink can help the system to stay below a value instead of going to an equilibrium point with very high amplitude. This result is illustrated by two numerical examples. The first one shows that even if the initial amplitude of the angle of the pendulum without absorber is very low, the system can reach very high amplitude. As shown in the second example, this does not happen with a nonlinear absorber.

Acknowledgements

The authors would like to thank “La Région Auvergne-Rhône-Alpes” for supporting this work in the frame of the CALIPSO project 17 010971 01 - 15 713.

References

[1] H. Frahm, “Device for damping vibrations of bodies.,” Apr. 1911. US Patent 989,958.

[2] R. E. Roberson, “Synthesis of a nonlinear dynamic vibration absorber,” *Journal of the Franklin Institute*, vol. 254, pp. 205–220, Sept. 1952.

[3] G. Habib and G. Kerschen, “A principle of similarity for nonlinear vibration absorbers,” *Physica D: Nonlinear Phenomena*, vol. 332, pp. 1–8, Oct. 2016.

[4] O. Gendelman, L. I. Manevitch, A. F. Vakakis, and R. M’Closkey, “Energy Pumping in Nonlinear Mechanical Oscillators: Part I-Dynamics of the Underlying Hamiltonian Systems,” *Journal of Applied Mechanics*, vol. 68, no. 1, p. 34, 2001.

[5] A. F. Vakakis and O. Gendelman, “Energy Pumping in Nonlinear Mechanical Oscillators: Part II. Resonance Capture,” *Journal of Applied Mechanics*, vol. 68, no. 1, p. 42, 2001.

[6] H. Matsuhisa and M. Yasuda, “Dynamic vibration absorber for pendulum type structure,” Oct. 1995. US Patent 989,958.

[7] Y. Song, H. Sato, Y. Iwata, and T. Komatsuzaki, “The response of a dynamic vibration absorber system with a parametrically excited pendulum,” *Journal of Sound and Vibration*, vol. 259, pp. 747–759, Jan. 2003.

[8] G. Hurel, A. Ture Savadkoohi, and C.-H. Lamarque, “Nonlinear vibratory energy exchanges between a two degrees-of-freedom pendulum and a nonlinear absorber.,” *Journal of Engineering Mechanics*, 2019. (in press).

[9] G. Hurel, A. Ture Savadkoohi, and C.-H. Lamarque, “Passive control of a two degrees-of-freedom pendulum by a non-smooth absorber,” *Nonlinear Dynamics*, 2019. (in press).

[10] L. I. Manevitch, “The Description of Localized Normal Modes in a Chain of Nonlinear Coupled Oscillators Using Complex Variables,” *Nonlinear Dynamics*, vol. 25, pp. 95–109, July 2001.

[11] A. Ture Savadkoohi, C.-H. Lamarque, M. Weiss, B. Vaurigaud, and S. Charlemagne, “Analysis of the 1:1 resonant energy exchanges between coupled oscillators with rheologies,” *Nonlinear Dynamics*, vol. 86, pp. 2145–2159, Dec. 2016.